Abrupt growth of large aggregates by correlated coalescences in turbulent flow

Jérémie Bec,[1] Samriddhi Sankar Ray,[2] Ewe Wei Saw,[1,3] and Holger Homann[1]

[1]*Laboratoire J.-L. Lagrange, Université Côte d'Azur, OCA, CNRS, Bd. de l'Observatoire, 06300 Nice, France*
[2]*International Centre for Theoretical Sciences, Tata Institute of Fundamental Research, Bangalore 560012, India*
[3]*Laboratoire SPHYNX, SPEC, CEA Saclay, CNRS, 91191 Gif-sur-Yvette, France*

Smoluchowski's coagulation kinetics is here shown to fail when the coalescing species are dilute and transported by a turbulent flow. The intermittent Lagrangian motion involves correlated violent events that lead to an unexpected rapid occurrence of the largest particles. This new phenomena is here quantified in terms of the anomalous scaling of turbulent three-point motion, leading to significant corrections in macroscopic processes that are critically sensitive to the early-stage emergence of large embryonic aggregates, as in planet formation or rain precipitation.

The formation of planets in circumstellar disks [1,2] as well as the initiation of rain in warm clouds [3,4] involve the coalescence of small dilute bodies suspended in a highly turbulent flow. It is crucial, in both cases, to determine the speed at which the largest objects are formed. Massive planetary embryos or big raindrops decouple from the underlying flow and accrete smaller particles more efficiently [5–7]. They are, very likely, the precursors for a runaway growth and possibly trigger the full coagulation process. Turbulent fluctuations might be essential in the formation of such large objects [8,9] but their precise role is still far from being fully understood. Significant progress has been made in understanding the enhancement of kinetic collision kernels due to turbulence. It is important to recall two key mechanisms present in the particle dynamics: *preferential concentration* [10], giving rise to high densities, and the *sling effect* [11] or *caustic formation* [12], responsible for large velocity differences; both mechanisms enhance the rate at which particles approach each other [13,14]. Precise quantitative models accounting for these two effects require appreciating the influence of turbulence [15,16]. However, their origin is not directly related to turbulent fluctuations but rather comes from the inertia of the suspended particles and the resulting detachment of their trajectories from the flow. Their impact on collision rates can then be studied in simple random flow [17–19].

In this Rapid Communication we show that, by its own, turbulent transport speeds up the growth of large objects. In the Lagrangian evolution of fluid elements, scaling and geometry are tied up by nontrivial memory effects. These interdependencies lead to *intermittent multiscaling* properties of advected passive scalar fields [20,21]. In the context of growth by coagulation, as shown in this work, they are responsible for a power-law tail in the distribution of times between successive collisions, yielding intricate correlations in the sequence of coalescences experienced by individual particles. Turbulent transport is thus the limiting factor for the coagulation kinetics, in analogy with diffusion-limited cluster-cluster aggregation or ballistic agglomeration (see [22] for a review). Because of this turbulent effect, we find that the number of large objects grows as a power law at short times, with an exponent much smaller than the one obtained from kinetic population-balance approaches. The value of this exponent is expressed in terms of the anomalous scaling

exponent ζ_3 associated to the third-order correlations of an advected passive scalar.

To simplify the presentation, we focus on an initially monodisperse suspension consisting of n_1 monomers ① with mass m_1. The extension to polydisperse situations is straightforward. These particles evolve in a turbulent flow and might coalesce, summing up their masses, when they collide. This dynamics leads, after some time, to the formation of a broad spectrum of particle sizes. We denote by ⑦ those constituted of i monomers and thus with a mass $i \times m_1$. Our goal is to determine how fast the number $n_i(t)$ of particles ⑦ grows with time for $i > 1$. Simple population-balance considerations lead to

$$\dot{n}_i(t) = \frac{1}{2} \sum_{j=1}^{i-1} \mathcal{Q}_{i-j,j}(t) - \sum_{j=1}^{\infty} \mathcal{Q}_{i,j}(t), \tag{1}$$

where the dot denotes time derivative. $\mathcal{Q}_{i,j}(t)dt$ is the number of coalescences ⑦ + ⑦ occurring between times t and $t + dt$. The first term in the right-hand side, the source, accounts for the rate at which particles ⑦ are created. The second, the sink, handles the coalescences of such particles with all others. When $n_i(0) = 0$ (for $i > 1$), the global coalescence rate $\mathcal{Q}_{i,j}$ can be written in terms of the individual particle rate by summing over all the creations of ⑦'s

$$\mathcal{Q}_{i,j}(t) = \int_0^t \lambda_{i,j}(t - s|s)\, n_j(t)\, \dot{n}_i(s)ds. \tag{2}$$

$\lambda_{i,j}(\tau|s)$ is the rate at which a particle ⑦, created at time s, coalesce with a ⑦ at time $s + \tau$. For statistically steady particle dynamics, this quantity is independent of the creation time s and $\lambda_{i,j}(\tau|s) = \lambda_{i,j}(\tau)$. Also, this rate relates to the probability distribution $p_{i,j}(\tau)$ of the time to next collision, which is given by

$$p_{i,j}(\tau) = \lambda_{i,j}(\tau)e^{-\int_0^\tau \lambda_{i,j}(\tau')d\tau'}. \tag{3}$$

This is the distribution of waiting time associated to the nonhomogeneous Poisson process with rate $\lambda_{i,j}(\tau)$.

At sufficiently long times τ, the coalescence rate $\lambda_{i,j}(\tau)$ is expected to approach a finite limit $\lambda_{i,j}^\infty$. Successive collisions of a single particle then appear to be uncorrelated. They define a memoryless process and $p_{i,j}(\tau)$ tends to the exponential distribution with rate parameter $\lambda_{i,j}^\infty$. The population-balance

system (1)-(2) then reduces to

$$\dot{n}_i = \frac{1}{2} \sum_{j=1}^{i-1} \lambda_{i-j,j}^{\infty} \, n_{i-j} \, n_j - \sum_{j=1}^{\infty} \lambda_{i,j}^{\infty} \, n_i \, n_j. \tag{4}$$

This is the celebrated Smoluchowski coagulation equation [23]. The stationary rates $\lambda_{i,j}^{\infty}$ are usually referred to as the collection or coalescence kernels. The work cited above on particle inertia was actually devoted to estimating their dependence upon particle sizes and the turbulent fluctuations of the carrier flow. The kinetic model (4) leads to predictions concerning the short-time increase of the n_i's. At the early stages of particle growth, the number n_1 of monomers remains almost constant and creations are dominant in the population balance. We thus get $\dot{n}_2 \simeq \lambda_{1,1}^{\infty} n_1^2 / 2$, so that $n_2(t) \simeq n_1^2 \lambda_{1,1}^{\infty} t/2$. For the next size, we have $\dot{n}_3 \simeq \lambda_{1,2}^{\infty} n_1 n_2$ and thus $n_3(t) \simeq n_1^3 \lambda_{1,1}^{\infty} \lambda_{1,2}^{\infty} t^2/4$. We obtain recursively

$$n_i(t) \simeq n_1^i (t/t_i)^{i-1}, \tag{5}$$

where the times t_i are averages of the times $1/\lambda_{j,k}^{\infty}$ associated to the different combinations of coalescences $\textcircled{j} + \textcircled{k}$ that are necessary to form a particle $\textcircled{i}$. The consistency of the assumptions can be checked *a posteriori*: The creation terms in (4) are always $\propto t^{i-2}$ and thus prevail at short times over the dominant destruction term $\propto t^{i-1}$.

The main assumption leading to Smoluchowski kinetics (4) is a convergence of the coalescence rate to its limiting value $\lambda_{i,j}^{\infty}$ much faster than the evolution of n_i. This is ensured for instance when the particles are very dense. For explaining the formation of large particles in a dilute suspension, these time scales are in general not sufficiently separated. The sudden appearance of sizable aggregates requires a brisk sequence of coalescences that are very likely to be correlated to each other. When, in addition, the coalescing species are transported by a turbulent flow, such correlations speed up the growth of large particles.

A statistically steady turbulent flow involves interactions between eddies of various sizes, ranging from the integral scale L, where kinetic energy is injected at a rate ε, down to the dissipative scale $\eta = \nu^{3/4}/\varepsilon^{1/4}$ below which viscous damping dominates (ν denotes the kinematic viscosity of the fluid). The degree of turbulence grows with the extension of this spatial span and is measured by the Reynolds number $\mathrm{Re} = (L/\eta)^{4/3}$. The intermediate scales between η and L define the inertial range through which energy cascades with a rate ε. Dimensional arguments suggest that the velocity increments between two points separated by a distance r in the inertial range behave as $u_r \sim (\varepsilon r)^{1/3}$. Such a phenomenology, referred to as Kolmogorov 1941, is often enough for capturing the most significant effects of turbulent fluctuations; in reality the scaling properties display slight deviations, due to intermittency, from this dimensional prediction [24,25].

The breakdown of scale invariance is much more striking for mixing statistics, owing to the fact that turbulence mingles together fluid elements in a robust manner. This pops up with the presence of quasidiscontinuities in the Lagrangian map where materials originating from distinct regions of the flow are violently brought together [see Fig. 1 (left)]. The emergence of such *fronts* is due to the inertial-range roughness of
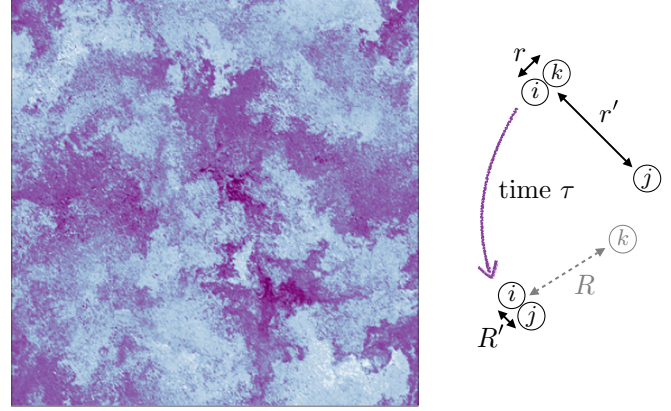

FIG. 1. Left: Distance traveled by fluid elements in a three-dimensional turbulent flow during one large-eddy turnover time. Long (white) and short (purple) distances, represented here as a function of the final position in a two-dimensional slice, define an intricate landscape with fronts where particles coming from far apart meet together. Right: Sketch of the event leading to correlated successive collisions. At the initial time (top), two particles i and k are located at a collision distance $r \lesssim \eta$, while a third one j is at distance $r' \gg \eta$ far from them. A time τ later (bottom) j has approached i at a distance $R' \lesssim \eta$ while k, having collided or not, has escaped to $R \gg \eta$.

the velocity field and the associated nonuniqueness of fluid element trajectories. Two initially separate tracers $\boldsymbol{x}_1(t)$ and $\boldsymbol{x}_2(t)$ that closely approach each other become indistinguishable and separate afterwards following Richardson's superdiffusion $|\boldsymbol{x}_1(t) - \boldsymbol{x}_2(t)|^2 \sim \varepsilon t^3$. Still, when interested in more than two fluid elements, this explosive behavior is constrained by the underlying presence of *statistical conservation laws* induced by the spatial correlations of the velocity field [20,21,26]. There exists specific functions of the shape and size of a cloud of n tracers that on average do not vary with time. Such zero modes are known to yield anomalous scaling in the statistics of an advected passive scalar θ. Its structure functions behave in the inertial range as $\langle (\theta(\boldsymbol{x} + \boldsymbol{r}) - \theta(\boldsymbol{x}))^n \rangle \sim |\boldsymbol{r}|^{n/3-\delta_n}$ where the discrepancies δ_n of the exponents from their dimensional prediction relate to the anomalous scaling of the transition probability of the distances between n tracers. As we will now see, the behavior of the three-point motion is in fact of relevance to coalescences.

In dilute suspensions, a coalescence results from two successive processes. First, the turbulent flow needs to bring two initially separate particles at a sufficiently close distance $\lesssim \eta$. Second, these close particles need to actually merge, and this involves various microphysical mechanisms (particle inertia, hydrodynamical interactions, surface effects). This leads us to write the coalescence rate as a product of two contributions:

$$\lambda_{i,j}(\tau) \approx \lambda_{i,j}^{\mathrm{turb}}(\tau) \times \lambda_{i,j}^{\mathrm{micro}}. \tag{6}$$

The contribution from turbulent transport can be written

$$\lambda_{i,j}^{\mathrm{turb}}(\tau) \approx \int u_\eta \, p_3(R,\eta,\tau|\eta,r',0)(r'^2/L^3) \, dr' \, dR \tag{7}$$

involving the transition probability p_3 of the three-point motion. More specifically, two successive collisions occur

if three particles [see Fig. 1 (right)], initially separated by distances $r = \eta$ and an arbitrary r', come in a time τ to distances R, arbitrary, and $R' = \eta$. The relation (7) is obtained by integrating over all possible initial distances r' of the particle ⓘ from the particle ⓙ, with a weight $\propto r'^2$ given by a uniform three-dimensional spatial distribution. The three tracers ⓘ, ⓙ, and ⓚ undergo in a time τ an evolution from a degenerate triangle with $r \ll r'$ to another degenerate triangle with, this time, $R \gg R'$. In turbulence, the probability transition between such configurations can be written as

$$p_3(R,R',\tau | r,r',0) \approx \left(\frac{\eta}{r'}\right)^2 \left(\frac{L}{r'}\right)^{\delta_3} \frac{1}{\varepsilon\tau^3} \Psi\left(\frac{r'^2}{\varepsilon\tau^3}, \frac{R^2}{\varepsilon\tau^3}\right),$$

where δ_3 is the anomalous part of the scaling exponent associated to the third-order statistics of an advected passive scalar; its value is universal (independent of the injection mechanism) and ≈ 0.18, as reported from several experimental and numerical studies [27]. In the expression above the first factor comes from integration over angles and can be seen as a small solid-angle contribution. The second factor originates from intermittency and gives a dependence upon the integral scale L. Physically, it means that when $\delta_3 > 0$, the closer is the third particle, the more likely it is to approach one of the other two. The last terms involve a dimensionless function Ψ that imposes Richardson's scaling for backward and forward pair evolution. This specific form of the three-point transition probability leads to

$$\lambda_{i,j}^{\text{turb}}(\tau) \propto \frac{\nu^{7/4}}{\varepsilon^{1/4} L^{3-\delta_3}} \int \Psi\left(\frac{r'^2}{\varepsilon\tau^3}, \frac{R^2}{\varepsilon\tau^3}\right) \frac{dr'\,dR}{r'^{\delta_3}\varepsilon\tau^3}$$

$$\propto (1/\tau_L)(\tau/\tau_L)^{-(3/2)\delta_3}, \qquad (8)$$

where $\tau_L = \varepsilon^{-1/3} L^{2/3}$ is the large-eddy turnover time (see Supplemental Material, Sec. B [28]). Turbulent transport thus leads to a power-law dependence in time of the coalescence rate. The associated distribution $p_{i,j}(\tau)$ of waiting time between successive collisions of a given particle is thus given by the Weibull distribution with shape parameter $1 - (3/2)\delta_3$. Plugging this behavior in the global coalescence rate (2) and by using the population-balance equations (1), one obtains a short-time behavior of the number of particles ⓘ that reads

$$n_i(t) \simeq n_1^i (t/\tilde{t}_i)^{[1-(3/2)\delta_3](i-2)+1}. \qquad (9)$$

Here the characteristic times $\tilde{t}_i$ are $\propto i\tau_L$, with a proportionality constant that involves the various microphysical rates $\lambda_{j,k}^{\text{micro}}$ of the coalescences leading to ⓘ. For $\delta_3 > 0$ the algebraic exponent appearing in (9) is smaller than that obtained in (5) from Smoluchowski's kinetics. The intermittency of turbulence mixing is thus enhancing the short-time growth by coalescence. In addition, the larger the aggregate size considered, the stronger this enhancement. Indeed, when i is large and $t \ll i\tau_L$, the formation of a particle ⓘ requires a large number of correlated coalescences separated by inertial-range times and the population dynamics is dominated by (9).

In order to corroborate our theoretical predictions on the enhancement of coalescences by turbulent mixing, we have performed direct numerical simulations for the evolution of a dilute population suspended in a turbulent flow. We start from one billion inertial point particles whose dynamics is given by
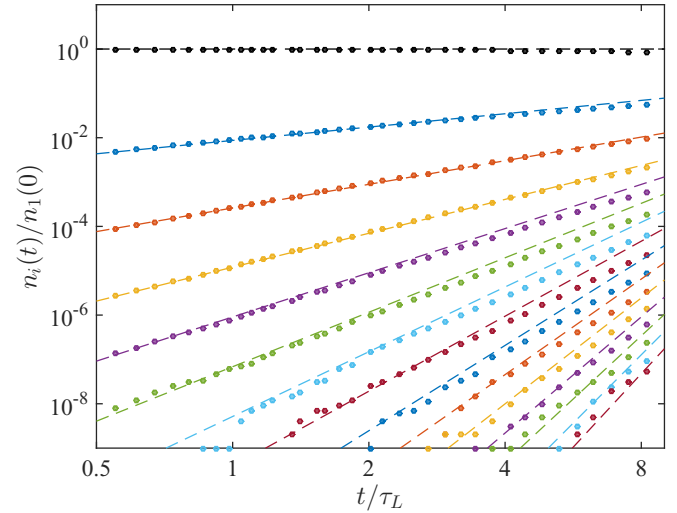

FIG. 2. Time evolution of the number $n_i(t)$ of particles [normalized by the initial number of monomers $n_1(0)$]; the mass i increases from 1 to 15 from top to bottom. The dots are the results of direct numerical simulations and the dashed lines show for $i \geqslant 2$ behaviors $\propto t^{0.73(i-2)+1}$ deduced from (9) for $\delta_3 = 0.18$.

a viscous Stokes drag:

$$\ddot{\boldsymbol{x}}_n = -\frac{1}{\tau_n}[\dot{\boldsymbol{x}}_n - \boldsymbol{u}(\boldsymbol{x}_n, t)], \qquad (10)$$

where $\boldsymbol{u}$ designates the fluid velocity field. It is obtained numerically by a pseudospectral integration of the incompressible Navier-Stokes equation using 2048^3 grid points. A large-scale forcing is applied in order to maintain the flow in a developed turbulent state with Re $\approx 50\,000$.

The particles follow the flow with a time lag given by their individual response times τ_n. Each particle has a virtual radius $a_n(t)$ and $\tau_n \propto a_n^2$. We start from a monodisperse suspension with monomers having initially all the same radius $a_i(0) = a_0 \approx \eta/10$. When two particles approach at a distance equal to the sum of their radii (detected using a billiard algorithm), they merge, conserving mass and momentum. Particles inertia is measured by their Stokes numbers $\text{St}_n = \tau_n \varepsilon^{1/2}/\nu^{1/2}$, which is initially small $\text{St}_n(0) \approx 0.1$. Inertia effects can thus be clearly neglected when interested in inertial-range length or time scales. The suspension is dilute: their volume fraction is approximately 5×10^{-5}, which represents in our flow one particle for each cube of volume $10\eta^3$ and is consistent with, for example, typical settings in a warm cloud of our atmosphere (see Supplemental Material, Sec. A [28]).

Figure 2 shows on log-log scales the time evolution of the number $n_i(t)$ of particles made from the merger of i monomers [that is, with radius $a(t) = i^{1/3} a_0$] for $i = 1, 2, \ldots 15$. Data (dots) are approximated very well by $n_i(t) \propto t^{0.73(i-2)+1}$ (dashed lines), corresponding to the predicted power laws (9) with $\delta_3 = 0.18$. Such a behavior persists for times larger than the large-eddy turnover time. The result of our simulation confirms the accuracy and the relevance of the predictions made earlier in this Rapid Communication. Large aggregates are appearing faster than predicted from kinetic models.

To confirm that this enhanced growth is indeed resulting from correlated successive collisions, we have measured the
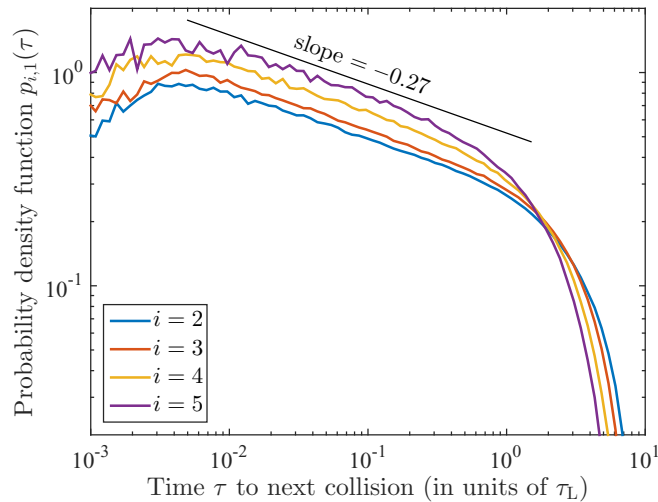
FIG. 3. Probability density function of the time between successive coalescences of a particle i with a monomer of mass 1. The power-law tail has, as we predict theoretically, an exponent $\approx -0.27 \approx -(3/2)\delta_3$.

probability density $p_{i,1}(\tau)$ of the time lag τ between the creation of a particle ⓘ and its next collision with a ①. Results are shown in Fig. 3 for $i = 2,3,4,5$. The distributions clearly display for τ in the inertial range a power-law decay, followed by a (stretched) exponential cutoff at $\tau \gtrsim \tau_L$. The measured value of the algebraic exponent is consistent with the predicted value $-(3/2)\delta_3 \approx -0.27$. This confirms that the intercollision time distribution follows (3) with a time-dependent coalescence rate $\lambda_{i,j}(\tau) \propto \tau^{-(3/2)\delta_3}$.

In conclusion, let us stress again that intermittency of turbulent mixing is responsible for an enhanced growth of dilute coalescing aggregates. The anomalous scaling properties, which are involved here, stem from the flow roughness in the turbulent inertial range and are expected to be also at play in the two-dimensional inverse cascade and in any random scale-invariant flows. Here, only third-order statistics are relevant since successive binary collisions involve the evolution of triplets of tracers that form degenerate triangles. Higher-order statistics enter other configurations (when, for instance, two particles are simultaneously formed and then merge) but they give subleading contributions. Finally, it is worth mentioning that the effect unveiled here might be accounted for by modifying kinetic models. When coarse-graining the population dynamics on sufficiently large time scales, correlated successive collisions will then appear as simultaneous multiple collisions.

[1] S. Weidenschilling and J. N. Cuzzi, *Protostars and Planets III* (University of Arizona Press, Tucson, 1993), Vol. 1, pp. 1031–1060.

[2] J. J. Lissauer, Ann. Rev. Astron. Astrophys. **31**, 129 (1993).

[3] M. Pinsky and A. Khain, J. Aerosol Sci. **28**, 1177 (1997).

[4] R. Shaw, Annu. Rev. Fluid Mech. **35**, 183 (2003).

[5] G. Wetherill and G. R. Stewart, Icarus **77**, 330 (1989).

[6] A. B. Kostinski and R. A. Shaw, Bull. Am. Meterol. Soc. **86**, 235 (2005).

[7] A. Johansen, M.-M. Mac Low, P. Lacerda, and M. Bizzarro, Sci. Adv. **1**, e1500109 (2015).

[8] A. Johansen, J. S. Oishi, M.-M. Mac Low, H. Klahr, T. Henning, and A. Youdin, Nature (London) **448**, 1022 (2007).

[9] E. Bodenschatz, S. Malinowski, R. Shaw, and F. Stratmann, Science **327**, 970 (2010).

[10] S. Sundaram and L. Collins, J. Fluid Mech. **335**, 75 (1997).

[11] G. Falkovich, A. Fouxon, and M. G. Stepanov, Nature (London) **419**, 151 (2002).

[12] M. Wilkinson, B. Mehlig, and V. Bezuglyy, Phys. Rev. Lett. **97**, 048501 (2006).

[13] W. Reade and L. Collins, J. Fluid Mech. **415**, 45 (2000).

[14] L.-P. Wang, B. Rosa, H. Gao, G. He, and G. Jin, Int. J. Multiphase Flow **35**, 854 (2009).

[15] B. Devenish *et al.*, Q. J. R. Meteorol. Soc. **138**, 1401 (2012).

[16] L. Pan and P. Padoan, Astrophys. J. **797**, 101 (2014).

[17] J. Bec, A. Celani, M. Cencini, and S. Musacchio, Phys. Fluids **17**, 073301 (2005).

[18] K. Gustavsson and B. Mehlig, Phys. Rev. E **87**, 023016 (2013).

[19] M. Voßkuhle, A. Pumir, E. Lévêque, and M. Wilkinson, J. Fluid Mech. **749**, 841 (2014).

[20] B. I. Shraiman and E. D. Siggia, Nature (London) **405**, 639 (2000).

[21] G. Falkovich, K. Gawędzki, and M. Vergassola, Rev. Mod. Phys. **73**, 913 (2001).

[22] F. Leyvraz, Phys. Rep. **383**, 95 (2003).

[23] M. von Smoluchowski, Z. Phys. Chem. **92**, 129 (1917).

[24] U. Frisch, *Turbulence* (Cambridge University Press, Cambridge, England, 1995).

[25] G. Falkovich and K. R. Sreenivasan, Phys. Today **59**(4), 43 (2006).

[26] I. Arad, L. Biferale, A. Celani, I. Procaccia, and M. Vergassola, Phys. Rev. Lett. **87**, 164502 (2001).

[27] Z. Warhaft, Ann. Rev. Fluid Mech. **32**, 203 (2000).

[28] See Supplemental Material at http://link.aps.org/supplemental/10.1103/PhysRevE.93.031102 for a detailed derivation of the above equations (in Sec. B); see Sec. A for details of the numerical simulation.